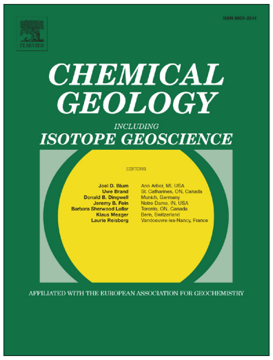

Potassium isotope fractionation during magmatic differentiation of basalt to rhyolite

Brenna Tuller-Ross, Paul S. Savage, Heng Chen, Kun Wang

PII: S0009-2541(19)30337-7
DOI: https://doi.org/10.1016/j.chemgeo.2019.07.017
Reference: CHEMGE 19242

To appear in: *Chemical Geology*

Received date: 11 March 2019
Revised date: 8 July 2019
Accepted date: 10 July 2019

Please cite this article as: B. Tuller-Ross, P.S. Savage, H. Chen, et al., Potassium isotope fractionation during magmatic differentiation of basalt to rhyolite, Chemical Geology, https://doi.org/10.1016/j.chemgeo.2019.07.017

Title: Potassium Isotope Fractionation During Magmatic Differentiation of Basalt to Rhyolite

Authors: Brenna Tuller-Ross[1]*, Paul S. Savage[2], Heng Chen[1], and Kun Wang(王昆)[1]

Affiliations:

[1] Department of Earth and Planetary Sciences and McDonnell Center for the Space Sciences, Washington University in St. Louis, MO 63130, USA.

[2] School of Earth and Environmental Sciences, University of St Andrews, St Andrews KY16 9AJ, UK.

* Correspondence authors' emails: brenna@wustl.edu; wangkun@wustl.edu

Keyword: Potassium Isotopes; MC-ICP-MS; Hekla; Magmatic differentiation; Isotope fractionation.

Manuscript prepared for Chemical Geology

Abstract:

High-temperature equilibrium and kinetic stable isotope fractionation during partial melting, fractional crystallization, and other igneous differentiation processes has been observed in many isotope systems, but due to the relative nascence of high-precision analytical capabilities for K, it is still unclear whether igneous processes induce systematic and resolvable K isotope fractionation. In this study, we look to the natural laboratory of Hekla volcano in Iceland to investigate the behavior of K isotopes during magmatic differentiation of basalt to rhyolite. Using a novel MC-ICP-MS method, we analyzed 24 geochemically diverse samples from Hekla, including 7 basalts, 8 basaltic andesites, 3 andesites, 4 dacites, and 2 rhyolites, along with 2 additional samples from Burfell, Iceland, for comparison (1 basalt and 1 trachyte). We observed extremely limited variation of $^{41}K/^{39}K$ ratios throughout our suite of samples, which is not resolvable within the best current analytical uncertainty. The average value of all samples is $\delta^{41}K_{NIST\ SRM3141a} = -0.46 \pm 0.07‰$ (2sd). This value agrees with the Bulk Silicate Earth value previously defined by average global oceanic basalts in literature. The lack of variation throughout this suite of samples from a single volcano system indicates that K does not fractionate during magmatic differentiation (of basalt to rhyolite) through processes such as partial melting and fractional crystallization. This conclusion is important to the estimation of the Bulk Silicate Earth K isotope composition, to placing a more robust estimate on the composition bulk continental crust, and to fostering a better understanding of the behavior of K isotopes during differentiation of the terrestrial planets.

1 Introduction

Potassium (K) is an incompatible lithophile, fluid-mobile alkali metal element. It is the eighth most abundant element in the Earth's crust and fifteenth most abundant element in the bulk Earth (McDonough and Sun, 1995; Rudnick and Gao, 2003). Its two stable isotopes, ^{39}K (abundance 93.26%) and ^{41}K (abundance 6.73%) have in recent years been used in a number of isotopic investigations into terrestrial and planetary phenomena, ranging from the investigation of the volatile-poor nature of Earth and Moon to applications of K in tracing seafloor alteration and subduction (e.g., Humayun and Clayton, 1995a, 1995b; Li et al., 2016; Morgan et al., 2018; Parendo et al., 2017a; Santiago Ramos et al., 2018; Wang and Jacobsen, 2016a, 2016b). Despite the potential of using K isotopes to explore problems in the geosciences, there are still many unknowns about this system due to the analytical difficulties of measuring K isotopes accurately. One of these primary unknowns, and the subject of this study, is whether or not K isotopes fractionate during magmatic differentiation. In addition, whether kinetic K isotope fractionation can occur during volcanic degassing is still unknown.

Since isotopic fractionation is a function of $1/T^2$ (Bigeleisen and Mayer, 1947), the magnitude of equilibrium stable isotopic fractionation occurring during high-temperature igneous processes is predicted to be small, normally on the sub-permille (‰) scale (e.g., Schauble, 2004). However, with the improvement of analytical precision (particularly linked to the application of MC-ICP-MS), studies of stable isotope systems in the past decade have shown that small degrees of isotopic fractionation do occur during magmatic differentiation (e.g., Johnson et al., 2004; Teng et al., 2017). For example, Si isotopes (^{30}Si/^{28}Si) have been shown to fractionate by up to ~0.20‰ during magmatic differentiation (Savage et al., 2011), Fe isotopes (^{56}Fe/^{54}Fe) have been observed to fractionate by ~0.15‰ (Schuessler et al., 2009; Teng et al., 2013) up to ~0.71‰ in mantle xenoliths (Zhao et al., 2017), and Zn (^{66}Zn/^{64}Zn) can fractionate by up to ~0.10‰ during partial melting and crystallization (Chen et al., 2013). Conversely, studies of other isotope systems such as Mg, Mo and Rb have shown no detectable whole-rock isotopic variations as a result of high-temperature igneous processes (Yang et al., 2015; Pringle and Moynier, 2017; Teng et al., 2013b). Establishing how a non-traditional stable isotope system (such as that of K) is affected during igneous processes is an important part of building the framework of understanding within which we can successfully apply each isotope system to problems in the geosciences.

Historically, the K isotope system was extensively investigated by Humayun and Clayton (1995a,b); they found no resolvable K isotope fractionation among any terrestrial samples within their analytical precision (±0.5‰; 2sd). However, as analytical methods and thus, precision, have improved over time, this conclusion has been revised. Specifically, improved precision (down to ±0.05‰; 2sd) using the Multiple-Collector Inductively-Coupled-Plasma Mass-Spectrometer (MC-ICP-MS) has indicated that there are significant variations (>1‰) in K isotope composition between terrestrial samples (Hu et al., 2018; Li et al., 2016; Morgan et al., 2018; Wang and Jacobsen, 2016a,b). Within this range, limited isotope variation has been observed among petrogenetically and geographically unrelated terrestrial igneous rocks (mostly geostandards) other than fluid-influenced pegmatites (Morgan et al., 2018), which hints that there is no fractionation of K isotopes during igneous differentiation. Further evidence in support of this supposition was reported by Tuller-Ross et al. (2019) wherein no statistically significant difference in K isotopic composition was found between 49 globally sourced basalts from different tectonic settings (mid-ocean ridge, oceanic island, and back-arc basin basalts; MORB, OIB and BABB), and no trend was observed between K isotopic composition and the (albeit limited range of) SiO_2 or K_2O concentrations in these basalts.

Until now there has been no study which explicitly explores the potential of K isotopic fractionation as a result of igneous processes. In order to investigate the magnitude (if any) of K isotopic fractionation as a result of magmatic differentiation, here we report the K isotopic compositions of a set of samples from Hekla volcano in Iceland. This locality has been utilized as an ideal natural laboratory for investigating “igneous” isotopic fractionation for other non-traditional isotope systems (e.g., Chen et al., 2013; Prytulak et al., 2017a; Savage et al., 2011; Schuessler et al., 2009; Yang et al., 2015) because this volcanic center produces volcanic material with a wide range of compositions (basalt through rhyolite) from one volcano, which should eliminate any location-based variables when comparing results.

2 Geologic background and sample description

Hekla, an active fissure volcano in the South Iceland Volcanic Zone is, on an anthropological timescale, one of the most active Icelandic volcanoes. There have been ~20 recorded historic eruptions since 1104 A.D., the most recent of which occurred in February, 2000 (Höskuldsson et al., 2007), as well as several prehistoric eruptions. Hekla is an unusual volcano in that it produces a broad range of volcanic products, from basalt to basaltic andesite, andesite, dacite, and rhyolite. Additionally, prior studies have established that there is no large-scale hydrothermal system associated with volcanic activity at Hekla and that contamination from geothermal fluids and crustal material is limited or absent (Sigmarsson et al., 1992; Thirlwall et al., 2006). Furthermore, lithium isotope data from Schuessler et al. (2009) suggests that chemical alteration from the exsolution of melt fluids can be excluded from consideration of differentiation processes at Hekla. Thus, any significant isotopic fractionation within Hekla material should be primarily the result of high-temperature igneous processes, which makes Hekla samples ideal for testing isotopic fractionation during magmatic differentiation.

Several petrogenetic models for Hekla magmas have been proposed. In the “classic” model by Sigmarsson et al. (1992), there exists a zoned magma chamber wherein magmas are both evolving and mixing: basaltic magma evolves by fractional crystallization into basaltic andesite magma; meanwhile, the partial melting of metabasic rocks by the basaltic magma as it rises through the Icelandic crust forms a dacitic melt. Some of this dacitic magma then continues to evolve via fractional crystallization, producing rhyolites, and some mixes with the basaltic andesite magma to form andesites. Thus, Sigmarsson et al. (1992) proposed a relatively simple petrogenetic model wherein magma undergoes two regimes of fractional crystallization (from $SiO_2 < 55\%$ and $SiO_2 > 67\%$) and one mixing regime ($55\% > SiO_2 < 67\%$) in a large (20 km long by 5 km wide by 7 km deep) magma chamber at a depth of roughly 8 km below the surface. Chekol et al. (2011) proposed a slightly modified model, wherein a large basaltic magma reservoir exists much deeper (near the crust-mantle interface), from which basaltic and basaltic andesite magmas rise to occupy multiple, smaller, separate magma pockets at shallower depths. Magmas in these pockets then undergo differentiation via crustal assimilation and fractional crystallization. The Chekol model is supported by the seeming lack of a shallow, large magma chamber when the Hekla subsurface is imaged by seismic methods (e.g., Soosalu and Einarsson, 2004) though it is possible that the models are not mutually exclusive, especially when considered over large timescales.

The samples used in this investigation are from the suite collected by Savage et al. (2011) between 2009 and 2010 (**Figure 1**). Of the 26 samples analyzed, 24 are from Hekla, and 2 are unrelated Icelandic volcanic samples (BUR20-09 and RHY01-09, both from near Burfell, Iceland) included for reference. All samples are either aphyric lava or tephra (**Table 1**). Overall, our suite of materials included 26 bulk samples: 8 basalts, 8 basaltic andesites, 3 andesites, 4 dacitic tephras, 2 rhyolitic tephras, and 1 trachyte; when plotted on a total alkali-silica (TAS) diagram, the samples show a clear transitional alkali series spanning SiO_2 contents of 46% to 72% (**Figure A1**). Major- and selected trace-elemental data is reported in Savage et al. (2011) and coincides with the range of compositions recorded in prior studies of Hekla rocks (e.g. Sigmarsson et al., 1992), and illustrates the broad range in composition represented in this sample suite (see **Figure 2**). In addition to these 26 Icelandic volcanic samples, we also repeatedly measured one USGS basaltic geostandard, BHVO-2 from Hawaii, to serve as the external standard during each analytical session.

3 Analytical Methods

The analytical method used in this study is reported in greater detail in Chen et al. (2019) and is similar to methods reported by other groups (Hu et al., 2018; Li et al., 2016; Morgan et al., 2018; Tian et al., 2018; Wang and Jacobsen, 2016a). Our 26 samples were prepared and analyzed in four steps: (1) digestion in acid; (2) purification using ion-exchange chromatography; (3) iCapQ quadrupole ICP-MS concentration and matrix analysis; and (4) isotope analysis with the Neptune Plus MC-ICP-MS.

3.1 Sample digestion

Samples were received in powdered form. First, the necessary mass of each sample (typically ~10mg) required for analysis was calculated using literature K_2O concentration data for the samples (Savage et al. 2011, 2010). The weight of each sample digested is listed in **Table 1**.

Each powdered sample was then dissolved in 6 mL of concentrated hydrofluoric acid (HF) and nitric acid (HNO_3) in a ratio of 3:1. Samples were digested in this acid solution under a heat lamp for a minimum of five days. After at least five days, the beakers were opened and the acid was allowed to evaporate. Once evaporated, 3 mL of 6N hydrochloric acid (HCl) was added to each beaker and samples were again left to digest under heat lamps. After at least 24 hours, beakers were opened and allowed evaporate one last time.

3.2 Ion-exchange chromatography to purify K

The method utilized to purify each sample for K was first proposed by Strelow et al. (1970) and is widely used in the contemporary study of potassium isotopes. Dried-down samples were re-dissolved in 1 mL of 0.7N HNO_3 and then were then run through one cycle of “big” and one cycle of “small” ion-exchange chromatography columns filled with 17 ml and 2.4 ml of BioRad AG50-X8 100-200 mesh cation-exchange resin, respectively. Columns were first rinsed with 100 mL or 20 mL 6N HCl for big or small columns, respectively. Samples were loaded and then eluted with 0.7N or 0.5N HNO_3 for big or small columns, respectively. Potassium was collected for each sample between 87 mL and 194 mL for big columns and between 16 mL and 34 mL for small columns. Several mL (5 for big columns, 2 for small columns) were collected immediately before and immediately after the K-cut volume to serve as pre- and post-cuts in asserting complete (>99%) collection of K. Process specifications are outlined in greater detail by Chen et al. (2019).

3.3 Elemental analysis with iCapQ ICP-MS

The K-cut for each sample was then analyzed against a multi-element standard using an iCapQ quadrupole ICP-MS (Thermo Scientific, Bremen, Germany) to determine if any matrix elements remained in the solution. In the event that any other element is present in the K-cut in amounts >1% relative to K, the sample is run through an additional cycle of small columns to avoid matrix effects. Pre- and post-cuts for each sample were also analyzed against the same multielement standard to check for any loss of K from the main K-cut. This ensures >99% recovery rate for K via ion exchange chromatography.

3.4 Isotopic analysis using MC-ICP-MS

The K concentrations acquired from iCapQ analysis were used to dilute each sample to match our K standard (300 ppb NIST SRM3141a) within 3%. Samples were then analyzed in the Neptune Plus MC-ICP-MS (Thermo Scientific, Bremen, Germany) in the Department of Earth and Planetary Sciences at Washington University in St Louis. Each sample was measured ~10 times via standard-sample bracketing; the average of the ~10 measurements are reported as each sample's δ^{41}K value, where $\delta^{41}K = [(^{41}K/^{39}K)_{sample}/(^{41}K/^{39}K)_{NIST\ SRM3141a} - 1]\times1000$ in units of per mil (‰). The analytical uncertainty was calculated as the 95% confidence interval (c.i.; see Table 1 footnotes) and it is given in Table 1 for each sample. One external standard, reference material BHVO-2, was used to monitor the data quality, and its measured values were consistent with reported values in literature (e.g. Chen et al., 2019; Hu et al., 2018; Li et al., 2016; Morgan et al., 2018; Wang and Jacobsen, 2016). Details about this method and long-term (20 months) reproducibility (~0.11‰, 2sd) are given in Chen et al. (2019).

4 Results

The K concentration and K isotope composition of each sample measured in this study are listed in **Table 1**. The K concentration of the same sample reported in literature is also listed for comparison. Our 26 total samples have K isotopic compositions ranging from –0.53± 0.03‰ to –0.41± 0.04‰. All samples have K isotopic values indistinguishable from each other within our long-term reproducibility (~0.11‰). Furthermore, a student's t-test performed on our data shows no statistically significant difference between δ^{41}K values for different rock types; average values for basalt (–0.46 ± 0.08, 2sd, n=8), basaltic andesite (–0.45 ± 0.07, 2sd, n=8), andesite (–0.43 ± 0.03, 2sd, n=3), dacite (–0.47 ± 0.07, 2sd, n=4), rhyolite (–0.49 ± 0.06, 2sd, n=2), and trachyte (–0.50 ± 0.05, n=1) are virtually indistinguishable from one another within uncertainties (**Figure 3**).

The samples overall have an average of –0.46 ± 0.07 (2sd) which is indistinguishable from the Bulk Silicate Earth (BSE) value defined by Wang and Jacobsen (2016a) of –0.48 ± 0.03‰ (2sd) using 3 basalts from different tectonic settings and is also indistinguishable from the updated BSE value defined by Tuller-Ross et al. (2019) of –0.43 ± 0.17‰ (2sd.) based on the average of 49 globally sourced MORBs, OIBs, and BABBs. This result agrees with previous studies of K isotopes measured in various igneous rocks (mostly geological standards) reported in literature (see **Figure 4b**). This study, however, is the first to select a suite of samples that are genetically related, i.e. taken from the same volcanic edifice and known to be chemically linked via igneous processes.

5 Discussion

5.1 Lack of K isotopic fractionation during magmatic differentiation

Hekla volcanic rocks provide us with the unique opportunity to study isotopic fractionation during magmatic differentiation because 1) they are derived from a single volcano by partial melting, fractional crystallization, and crustal assimilation during fractional crystallization (Chekol et al., 2011; Sigmarsson et al., 1992), and 2) contamination from country rocks is not significant due to its similar composition, and 3) they have not been influenced by hydrothermal fluids (Chen et al., 2013; Schuessler et al., 2009). Therefore, any variation in isotopic composition occurring among Hekla samples should reflect isotopic fractionation during high temperature igneous processes rather than by source heterogeneity, country rock assimilation, or hydrothermal alteration.

Following this logic, studies of several isotope systems and their behavior during igneous differentiation have been investigated in Hekla samples (see **Figure 5**). While some isotope systems show no resolvable isotope fractionation at Hekla (**Figure 5a**), others (*e.g.* Si, Fe, V) show significant trends (**Figure 5b,c**). A previous study by Savage et al. (2011) on the same samples from Hekla shows that silicon isotopic compositions vary and correlate with SiO_2 content (**Figure 5b**); redox-sensitive isotope systems such as Fe (**Figure 5b**) and V (**Figure 5c**) also show systematic isotopic fractionations during fractional crystallization (Prytulak et al., 2017b; Schuessler et al., 2009). However, for Li, Zn, Mo, and Tl no resolvable and/or systematic isotopic variation has been found among the Hekla series of igneous rocks (**Figure 5a,c**) (Chen et al., 2013; Prytulak et al., 2017a; Schuessler et al., 2009; Yang et al., 2015).

For K isotopes, there is no clear trend or systematic variation in $\delta^{41}K$ values when plotted against concentration of SiO_2, K_2O, MgO, Ba, or Th (**Figure 5a**, **Figure 4**). As shown in **Figure 5** and discussed in Section 2 of this paper, Hekla samples are thought to be generated via two fractional crystallization regimes and one mixing regime (Sigmarsson et al., 1992), although there is some work that modifies this interpretation (e.g. Chekol et al., 2011). The ranges of K isotope composition observed within the two fractional crystallization regimes ($SiO_2 < 55\%$ and $SiO_2 >$

67%) are 0.12‰ and 0.10‰, respectively; the range observed within the mixing regime (55% < SiO_2 < 67%) is even smaller at 0.04‰. These ranges fall within our lab's long-term reproducibility of ±0.11‰ (Chen et al., 2019) and are not significantly over our typical within-run analytical uncertainties of ±0.05‰. This suggests that K isotopes are not significantly fractionated due to partial melting or mineral fractionation within the Hekla system. This observation is consistent with the theoretical consideration of K isotopic fractionation during magmatic differentiation: since K is highly incompatible, and as it has single valance, there is no redox effect. Given the strong correlation between K and Ba (**Figure 2a**) and K and Th (Figure 1c), major K-bearing mineral phases appear to be absent as liquidus phases crystallizing from the melt. In simple terms, if K is not being removed from the melt by a major mineral phase, there is no mass transfer of K from the melt and hence no isotope fractionation. However, in alkali-rich systems (such as nepheline syenites) we may begin to see K isotope fractionation due to K partitioning into K-bearing minerals (*e.g.*, Chen et al., 2019; Morgan et al. 2018); though, as such systems are relatively uncommon, their potential influence is not significant when considering bulk silicate reservoir values.

Based on the two observations that 1) the igneous differentiation process is the primary process that could lead to isotope fractionation at Hekla and 2) the data show no statistically significant variations in K isotopic composition between basalt, basaltic andesite, andesite, dacite, and rhyolite from one volcano system, we conclude that K does not fractionate during high-temperature igneous differentiation processes (especially in systems where K-bearing minerals are not modally important, i.e., in tholeiitic and transitional-alkaline systems). This is significant for two reasons: 1) If we assume that K isotopes do not fractionate during igneous differentiation, we can use the K isotopic compositions of unaltered igneous rocks to infer the K isotopic compositions of their sources (*e.g.*, mantle); and 2) We can use the K isotope compositions of unaltered igneous rocks for interplanetary comparison purposes.

5.2 Lack of K isotopic fractionation during volcanic degassing

Potassium is a moderately volatile element and its 50% condensation temperature is 1006K (Lodders, 2003), which is similar to that of chlorine (948K). Both field observations and thermodynamic calculations show that high-temperature volcanic gasses contain trace amount of potassium as KCl gas (Crowe et al., 1987; Pennisi et al., 1988; Symonds et al., 1994), and kinetic Cl isotope fractionation (up to +12‰) has been found to occur during volcanic degassing (Barnes et al., 2009; Eggenkamp, 1994; Sharp et al., 2010). Although K isotope compositions of volcanic gases have never been directly analyzed, during laboratory vaporization experiments large (up to +10‰) kinetic fractionation of K isotopes has been observed in the vaporization residues (Richter et al., 2011; Yu et al., 2003). Therefore, it is possible that volatile loss of K due to degassing during eruptions could fractionate K isotopes, and this effect must be evaluated for the Hekla volcanic rocks in this study.

Hekla lavas are known to undergo significant S (in the form of SO_4^{2-}), Cl, and F loss to degassing during eruptions (Moune et al., 2007). In their study of Zn isotopes, Chen et al. (2013) used S content as a proxy for degree of degassing and compared the Zn isotopic ratios of Hekla samples to their S content to investigate whether a correlation exists between degree of degassing and Zn isotope fractionation. They found that there was a slight negative trend (R^2=0.30) between δ^{66}Zn and S concentration. Here, we take the same approach (**Figure 5**), and find no significant correlation (slope=0.00014, R^2=0.03) between δ^{41}K and S concentration, suggesting that there is no *resolvable* K isotope fractionation due to kinetic fractionation during volatile loss at Hekla.

We can use K isotopes to constrain the maximum amount of K lost during volcanic degassing. The theoretical Rayleigh fractionation coefficient (α) during vaporization as KCl gas can be calculated as the square root of the mass difference of the ^{39}KCl and ^{41}KCl [$(74.4167/76.4148)^{0.5}$=0.9868]. However, such theoretical Rayleigh fractionation coefficients can be only applied to free evaporation in vacuum and is not relevant to real-world volcanic degassing. Yu et al. (2003) has experimentally calibrated Rayleigh fractionation coefficients through vaporizing a peralkaline silicate melt and obtained values between 0.9848 and 0.9912 at 1 bar pressure in air. Using the range of K isotope compositions among Hekla samples (~0.12‰), we can constrain the maximum amount of K lost during volcanic degassing of Hekla volcano to be less than 0.8-1.3%. Note that this is assuming the range of isotope compositions among Hekla samples is entirely caused by volcanic degassing instead of analytical uncertainty. This constraint is only to put an upper bound of the K volatile loss during Hekla volcanic degassing, and the percentage of K loss is likely much smaller.

5.3 Implications for K isotopic fractionation during the differentiation of the Earth

Due to the relatively recent development of high-precision K isotope analysis techniques, to date there have been only a limited number of high-precision studies aiming to constrain the K isotopic composition of different Earth reservoirs. Studies of K isotopes in terrestrial samples have thus far been largely limited to igneous rocks (e.g., Morgan et al., 2018; Wang and Jacobsen, 2016a) and samples altered by fluids (e.g., Morgan et al., 2018; Parendo et al., 2017; Santiago Ramos et al., 2018). Such studies have shown that materials altered by hydrothermal fluids can have K isotope compositions that vary significantly from the BSE average both positively and negatively. Overall, Morgan et al. (2018) found a ~2.6‰ variability in their suite of diverse geological samples (both low- and high-temperature) but notes that the only igneous samples varying significantly from the BSE value are pegmatites which have been subject to influence by fluids during late-stage crystallization. Pegmatites are also host to a number of phases containing high concentrations of incompatible elements, such as K, and fractionation of these phases has the potential to affect the K isotope composition of the remaining fluid/melt. Parendo et al. (2017) found a significant δ^{41}K divergence of ~0.7‰ from the BSE value in hydrothermally altered oceanic crust samples. Santiago-Ramos et al. (2018) observed δ^{41}K variations of up to ~1.8‰ in deep-sea sediment pore fluids. Similarly, Tuller-Ross et al. (in review) found that two (palagonite-bearing) OIB samples that had been visibly altered by aqueous processes had K isotopic compositions similar to that of seawater (~0.0‰) while the other 49 samples, which appeared pristine, had K isotopic compositions indistinguishable from the BSE within uncertainties.

Although sedimentary rocks and altered igneous rocks display large K isotopic variability, creating K isotopic heterogeneity within the crust and potentially in the mantle through subduction mechanisms (although not observed in MORB, OIB and BABB; Tuller-Ross et al., 2018), unaltered igneous rocks have shown limited K isotope variation and indicate that magmatic differentiation in general does not generate *measurable* K isotope fractionation. This observation is based on not only this suite of Hekla volcanic rocks (from basalts to rhyolites), but also all available data of bulk igneous rocks that have been analyzed to date (Hu et al., 2018; Li et al., 2016; Morgan et al., 2018; Tian et al., 2018; Wang and Jacobsen, 2016a). We do want to note that for more evolved (higher SiO_2 than andesitic or dacitic) igneous rocks, caution is needed as K-bearing phases will become more important during crystallization, which may possibly induce inter-mineral/melt-mineral isotopic fractionations; however, so far there is too little data to support such a hypothesis.

Considering that magmatic differentiation is one of the primary processes of planetary differentiation, we propose that (unaltered) crustal igneous rocks can be used to estimate the K isotopic composition of the Earth's mantle. **Figure 7** illustrates this idea and shows a hypothesized plot of K isotopic composition for different Earth reservoirs that are as of yet undefined for K isotopes. Different major Earth reservoirs such as the mantle and the lower, middle, upper continental crusts display a trend of increasing K concentration with progressing SiO_2 abundance due to the incompatibility of K during partial melting, which resembles the trend also shown among Hekla samples (see **Figure 7**). The lack of K isotopic fractionation between the melt and mineral phases during magmatic differentiation observed in the Hekla suite may be also applied to the greater suite of Earth major reservoirs. One must keep in mind that such a plot is looking at the *bulk* isotopic composition of K in the entire reservoir—ignoring the heterogeneity and fractionation *within* the reservoir. As shown in **Figure 7**, the overall K isotope composition of the bulk crust would be indistinguishable from that of the middle continental crust, lower continental crust, and mantle. This implication, if can be confirmed, could be significant for the purposes of interplanetary comparison and determining the bulk K compositions of other terrestrial bodies.

6 Conclusion

This study is the first documentation of the K isotopic composition of a suite of compositionally diverse igneous samples from one volcano system. Hekla volcano is an ideal natural laboratory, free of major contamination from country rock assimilation or hydrothermal influence. Although magmatic differentiation at Hekla produces a broad range of bulk chemical compositions spanning basalt to rhyolite, such diverse samples show no distinguishable K isotopic variability. We note that the volcanic degassing, a common fractionating process in volcano systems, does not appear to have an effect on K isotopes; nor does Soret diffusion, potentially ruling out the “classic” petrogenetic model at Hekla wherein all fractional crystallization and mixing occurs in a large magma chamber where a large thermal gradient would be expected. Most significantly, our results suggest that magmatic differentiation produces no measurable K isotopic fractionation in differentiated, volcanic materials relative to their source materials. Unaltered igneous rocks can thus be used to infer the K isotope compositions of their source, which makes it possible to estimate the bulk K isotopic compositions for the mantles of Earth and other planetary bodies (such as the Moon and Mars).

Acknowledgements

The authors thank Editor Dr. Catherine Chauvel and two anonymous reviewers for their thorough and constructive reviews. We also thank the McDonnell Center for the Space Sciences and the UK National Environment Research Council for their support. Funding for this work was provided in part by NERC grant NE/R002134/1.

References

Barnes, J.D., Sharp, Z.D., Fischer, T.P., Hilton, D.R., Carr, M.J., 2009. Chlorine isotope variations along the Central American volcanic front and back arc. Geochemistry, Geophys. Geosystems 10, n/a-n/a.

Bigeleisen, J., Mayer, M.G., 1947. Calculation of Equilibrium Constants for Isotopic Exchange Reactions. J. Chem. Phys. 15, 261–267.

Chekol, T.A., Kobayashi, K., Yokoyama, T., Sakaguchi, C., Nakamura, E., 2011. Timescales of magma differentiation from basalt to andesite beneath Hekla Volcano, Iceland: Constraints from U-series disequilibria in lavas from the last quarter-millennium flows. Geochim. Cosmochim. Acta 75, 256–283.

Chen, H., Savage, P.S., Teng, F.-Z., Helz, R.T., Moynier, F., 2013. Zinc isotope fractionation during magmatic differentiation and the isotopic composition of the bulk Earth. Earth Planet. Sci. Lett. 369–370, 34–42.

Chen, H., Tian, Z., Tuller-Ross, B., Korotev, R.L., Wang, K., 2019. High-precision potassium isotopic analysis by MC-ICP-MS: an inter-laboratory comparison and refined K atomic weight. J. Anal. At. Spectrom.

Crowe, B.M., Finnegan, D.L., Zoller, W.H., Boynton, W. V., 1987. Trace element geochemistry of volcanic gases and particles from 1983-1984 eruptive episodes of Kilauea Volcano. J. Geophys. Res. Solid Earth 92, 13708–13714.

Eggenkamp, H.G.M., 1994. The geochemistry of chlorine isotopes. Universiteit Utrecht.

Höskuldsson, Á., Óskarsson, N., Pedersen, R., Grönvold, K., Vogfjörð, K., Ólafsdóttir, R., 2007.

The millennium eruption of Hekla in February 2000. Bull. Volcanol. 70, 169–182.

Hu, Y., Chen, X., Xu, Y.-K., Teng, F.-Z., 2018. High-precision analysis of potassium isotopes by HR-MC-ICPMS. Chem. Geol. 493, 100–108.

Humayun, M., Clayton, R.N., 1995a. Potassium isotope cosmochemistry: Genetic implications of volatile element depletion. Geochim. Cosmochim. Acta 59, 2131–2148.

Humayun, M., Clayton, R.N., 1995b. Precise determination of the isotopic composition of potassium: Application to terrestrial rocks and lunar soils. Geochim. Cosmochim. Acta 59, 2115–2130.

Johnson, C.M., Beard, B.L., Albarede, F., 2004. Geochemistry of Non-Traditional Stable Isotopes, Reviews in Mineralogy and Geochemistry.

Li, W., Beard, B.L., Li, S., 2016. Precise measurement of stable potassium isotope ratios using a single focusing collision cell multi-collector ICP-MS. J. Anal. At. Spectrom. 31, 1023–1029.

Lodders, K., 2003. Solar System Abundances and Condensation Temperatures of the Elements. Astrophys. J. 591, 1220–1247.

McDonough, W.F., Sun, S. -s., 1995. The composition of the Earth. Chem. Geol. 120, 223–253.

Morgan, L.E., Santiago Ramos, D.P., Davidheiser-Kroll, B., Faithfull, J., Lloyd, N.S., Ellam, R.M., Higgins, J.A., 2018. High-precision41K/39K measurements by MC-ICP-MS indicate terrestrial variability of: δ41K. J. Anal. At. Spectrom. 33, 175–186.

Moune, S., Sigmarsson, O., Thordarson, T., Gauthier, P.-J., 2007. Recent volatile evolution in the magmatic system of Hekla volcano, Iceland. Earth Planet. Sci. Lett. 255, 373–389.

Parendo, C.A., Jacobsen, S.B., Wang, K., 2017. K isotopes as a tracer of seafloor hydrothermal alteration. Proc. Natl. Acad. Sci. U. S. A. 114, 1827–1831.

Pedersen, G.B.M., Montalvo, J., Einarsson, P., Vilmundardóttir, O., Sófus Sigurmundsson, F., Muñoz-Cobo Belart, J., Hjartardóttir, Á., Kizel, F., Rustowicz, R., Falco, N., Gísladóttir, G., Benediktsson, J., 2019. Historical lava flow fields at Hekla volcano, South Iceland. Jökull 68, 1–26.

Pennisi, M., Le Cloarec, M.F., Lambert, G., Le Roulley, J.C., 1988. Fractionation of metals in volcanic emissions. Earth Planet. Sci. Lett. 88, 284–288.

Pringle, E.A., Moynier, F., 2017. Rubidium isotopic composition of the Earth, meteorites, and the Moon: Evidence for the origin of volatile loss during planetary accretion. Earth Planet. Sci. Lett. 473, 62–70.

Prytulak, J., Brett, A., Webb, M., Plank, T., Rehkämper, M., Savage, P.S., Woodhead, J., 2017a. Thallium elemental behavior and stable isotope fractionation during magmatic processes. Chem. Geol. 448, 71–83.

Prytulak, J., Sossi, P.A., Halliday, A.N., Plank, T., Savage, P.S., Woodhead, J.D., 2017b. Stable vanadium isotopes as a redox proxy in magmatic systems? Geochemical Perspect. Lett. 75–84.

Richter, F.M., Mendybaev, R.A., Christensen, J.N., Ebel, D., Gaffney, A., 2011. Laboratory experiments bearing on the origin and evolution of olivine-rich chondrules. Meteorit. Planet. Sci. 46, 1152–1178.

Rudnick, R.L., Gao, S., 2003. Composition of the Continental Crust, in: Treatise on

Geochemistry. Elsevier, pp. 1–64.

Santiago Ramos, D., Morgan, L., Lloyd, N., Higgins, J., 2018. Reverse weathering in marine sediments and the geochemical cycle of potassium in seawater: Insights from the K isotopic composition (41 K/ 39 K) of deep-sea pore-fluids, Geochimica et Cosmochimica Acta.

Savage, P.S., Georg, R.B., Williams, H.M., Burton, K.W., Halliday, A.N., 2011. Silicon isotope fractionation during magmatic differentiation. Geochim. Cosmochim. Acta 75, 6124–6139.

Schauble, E.A., 2004. Applying Stable Isotope Fractionation Theory to New Systems. Rev. Mineral. Geochemistry 55, 65–111.

Schuessler, J.A., Schoenberg, R., Sigmarsson, O., 2009. Iron and lithium isotope systematics of the Hekla volcano, Iceland — Evidence for Fe isotope fractionation during magma differentiation. Chem. Geol. 258, 78–91.

Sharp, Z.D., Barnes, J.D., Fischer, T.P., Halick, M., 2010. An experimental determination of chlorine isotope fractionation in acid systems and applications to volcanic fumaroles. Geochim. Cosmochim. Acta 74, 264–273.

Sigmarsson, O., Condomines, M., Fourcade, S., 1992. A detailed Th, Sr and O isotope study of Hekla: differentiation processes in an Icelandic Volcano. Contrib. to Mineral. Petrol. 112, 20–34.

Soosalu, H., Einarsson, P., 2004. Seismic constraints on magma chambers at Hekla and Torfajökull volcanoes, Iceland. Bull. Volcanol. 66, 276–286.

Strelow, E.W.E., Von S. Toerien, F., Weinert, C.H.S.W., 1970. Accurate determination of traces of sodium and potassium in rocks by ion exchange followed by atomic absorption spectroscopy. Anal. Chim. Acta 50, 399–405.

Symonds, R.B., Rose, W.I., Bluth, G.J.S., Gerlack, T.M., 1994. Volcanic- gas studies: Methods, results, and applications, in: Carroll, M.R., Holloway, J.R. (Eds.), Volatiles in Magmas. Mineralogical Society America, pp. 1–66.

Teng, F.-Z., Dauphas, N., Huang, S., Marty, B., 2013. Iron isotopic systematics of oceanic basalts. Geochim. Cosmochim. Acta 107, 12–26.

Teng, F.-Z., Dauphas, N., Watkins, J.M., 2017. Non-Traditional Stable Isotopes, Reviews in Mineralogy and Geochemistry.

Teng, F.-Z., Li, W.-Y., Ke, S., Marty, B., Dauphas, N., Huang, S., Wu, F.-Y., Pourmand, A., 2010. Magnesium isotopic composition of the Earth and chondrites. Geochim. Cosmochim. Acta 74, 4150–4166.

Thirlwall, M.F., Gee, M.A.M., Lowry, D., Mattey, D.P., Murton, B.J., Taylor, R.N., 2006. Low δ18O in the Icelandic mantle and its origins: Evidence from Reykjanes Ridge and Icelandic lavas. Geochim. Cosmochim. Acta 70, 993–1019.

Tian, Z., Chen, H., Fegley, B., Lodders, K., Barrat, J.A., Wang, K., 2018. Potassium Isotope Differences Among Chondrites, Earth, Moon, Mars, and 4-Vesta — Implication on the Planet Accretion Mechanisms. 49th Lunar Planet. Sci. Conf. 19-23 March, 2018, held Woodlands, Texas LPI Contrib. No. 2083, id.1276 49.

Tomascak, P.B., Langmuir, C.H., le Roux, P.J., Shirey, S.B., 2008. Lithium isotopes in global mid-ocean ridge basalts. Geochim. Cosmochim. Acta 72, 1626–1637.

Tuller-Ross, B., Marty, B., Kelley, K.A., Chen, H., Wang, K., Lee, H., 2019. Potassium isotope systematics of oceanic basalts. Geochim. Cosmochim. Acta.

Wang, K., Jacobsen, S.B., 2016a. An estimate of the Bulk Silicate Earth potassium isotopic composition based on MC-ICPMS measurements of basalts. Geochim. Cosmochim. Acta 178, 223–232.

Wang, K., Jacobsen, S.B., 2016b. Potassium isotopic evidence for a high-energy giant impact origin of the Moon. Nature 538, 487–490.

Yang, J., Siebert, C., Barling, J., Savage, P., Liang, Y.-H., Halliday, A.N., 2015. Absence of molybdenum isotope fractionation during magmatic differentiation at Hekla volcano, Iceland. Geochim. Cosmochim. Acta 162, 126–136.

Yu, Y., Hewins, R.H., Alexander, C.M.O. ’D., Wang, J., 2003. Experimental study of evaporation and isotopic mass fractionation of potassium in silicate melts. Geochim. Cosmochim. Acta 67, 773–786.

Zhao, X., Zhang, Z., Huang, S., Liu, Y., Li, X., Zhang, H., 2017. Coupled extremely light Ca and Fe isotopes in peridotites. Geochim. Cosmochim. Acta 208, 368–380.

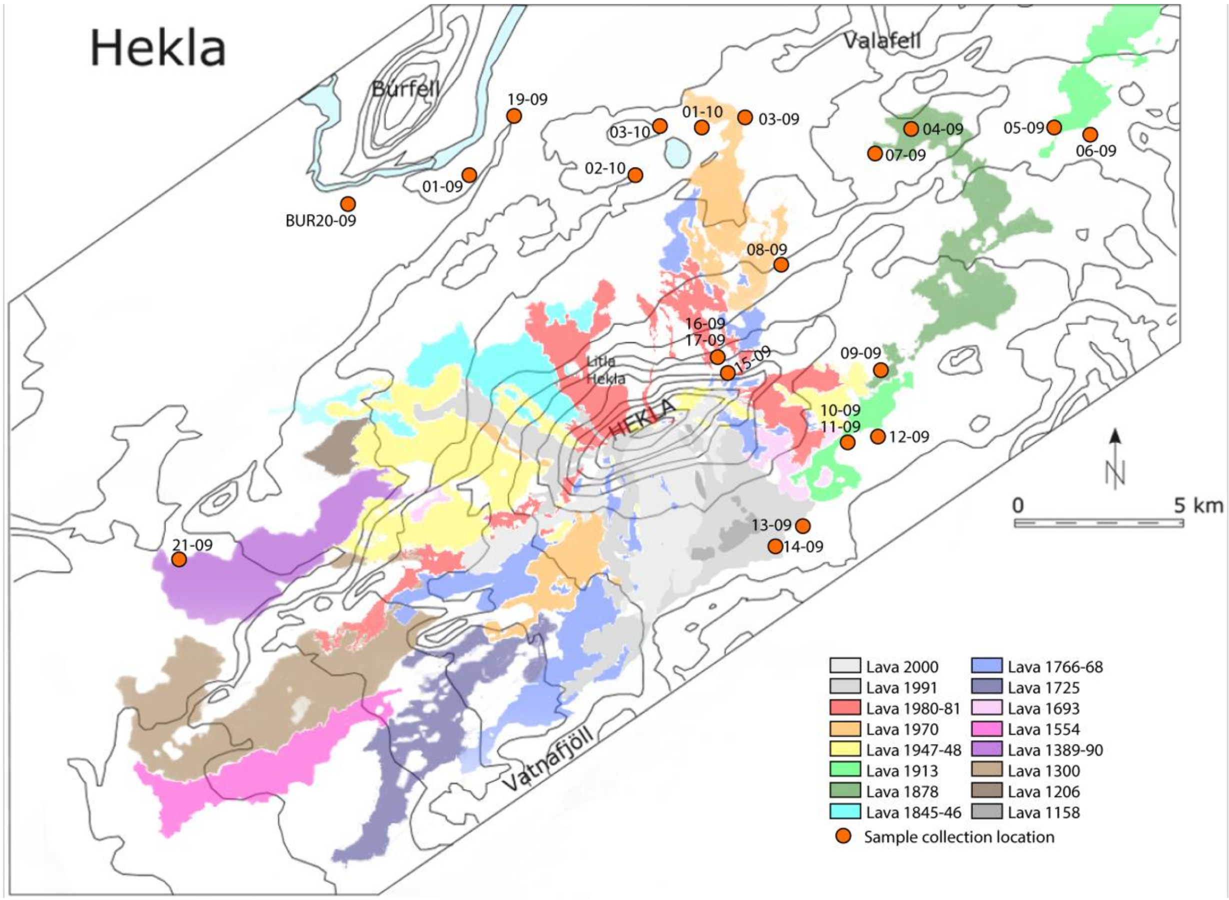

Figure 1: *Map showing collection locations of samples analyzed in this study. Lava flow data from Pedersen et al., 2019; topographic base map from Savage et al., 2011.*

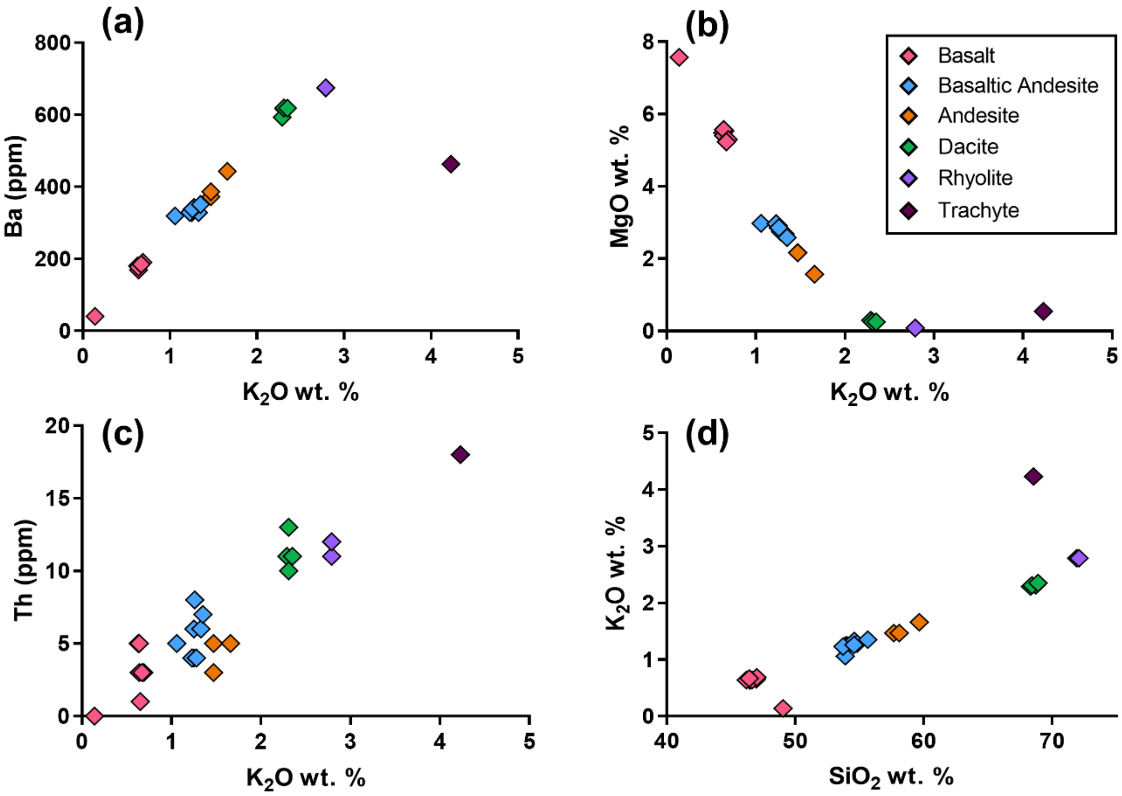

Figure 2: *The geochemical composition of the samples analyzed in this study. Panels show a) Barium versus K_2O wt%; b) MgO wt.% versus K_2O wt.%; c) Th versus K_2O wt.%; and d) K_2O wt% vs. SiO_2 wt.%. Ba, Th, and MgO data from Savage et al. (2011).*

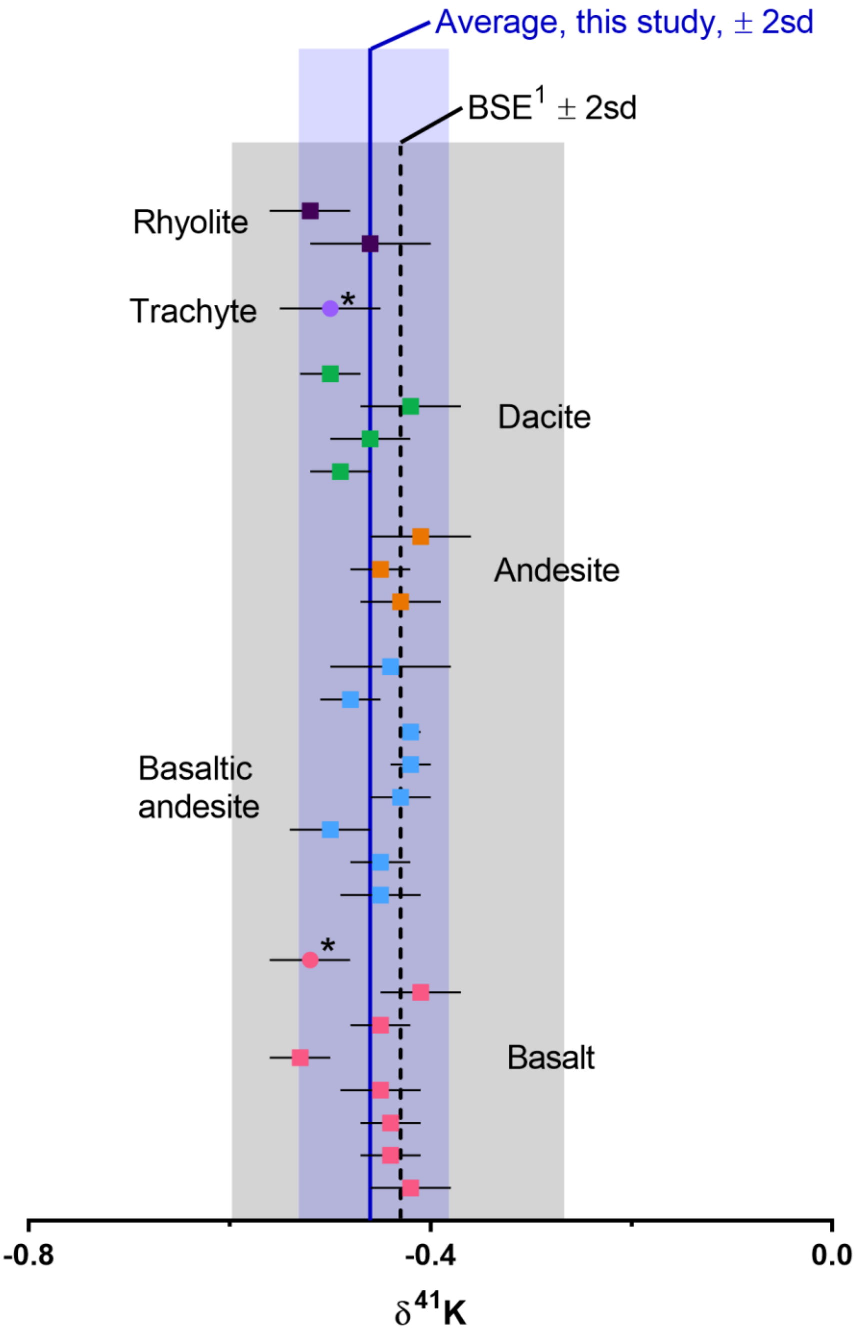

Figure 3: *All samples in this study plotted by sample group. The dashed black line and shaded gray area represents the BSE value of −0.43 ± 0.17 (2sd) from Tuller-Ross et al. (2019); the solid blue line and shaded blue area represents the average δ^{41}K of this study, −0.46 ± 0.07 (2sd). The 2 points marked with asterisks are BUR20-09 and RHY01-09, reference samples from Burfell, Iceland. Error bars are 95% c.i.*

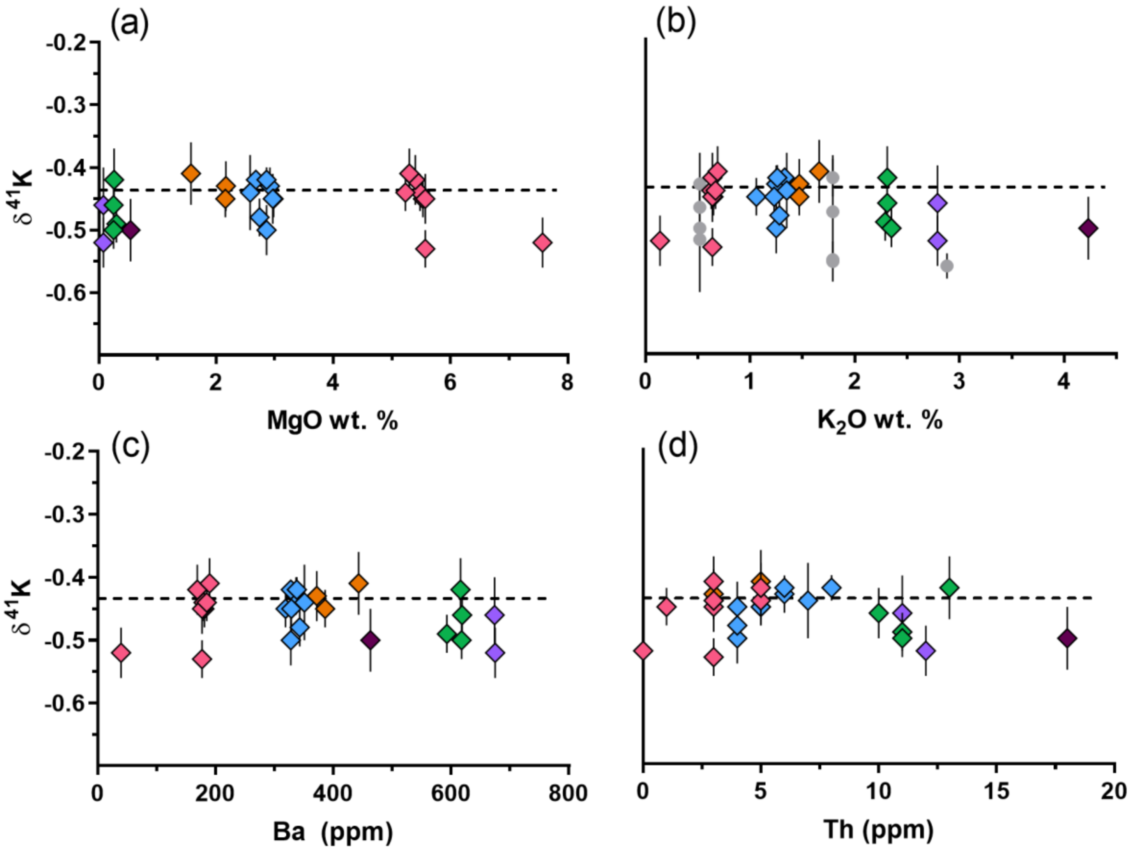

Figure 4: *K isotopic composition plotted against a) MgO wt.%; b) K$_2$O wt.%; c) Ba concentration; and d) Th concentration. The dashed line represents the BSE value given by Tuller-Ross et al. (2019). The gray points in panel (b) represent data for igneous USGS standards analyzed by other groups (Morgan et al. 2016; Hu et al, 2018; Li et al., 2016; Wang and Jacobsen, 2016a,b). Errors are 95% c.i.*

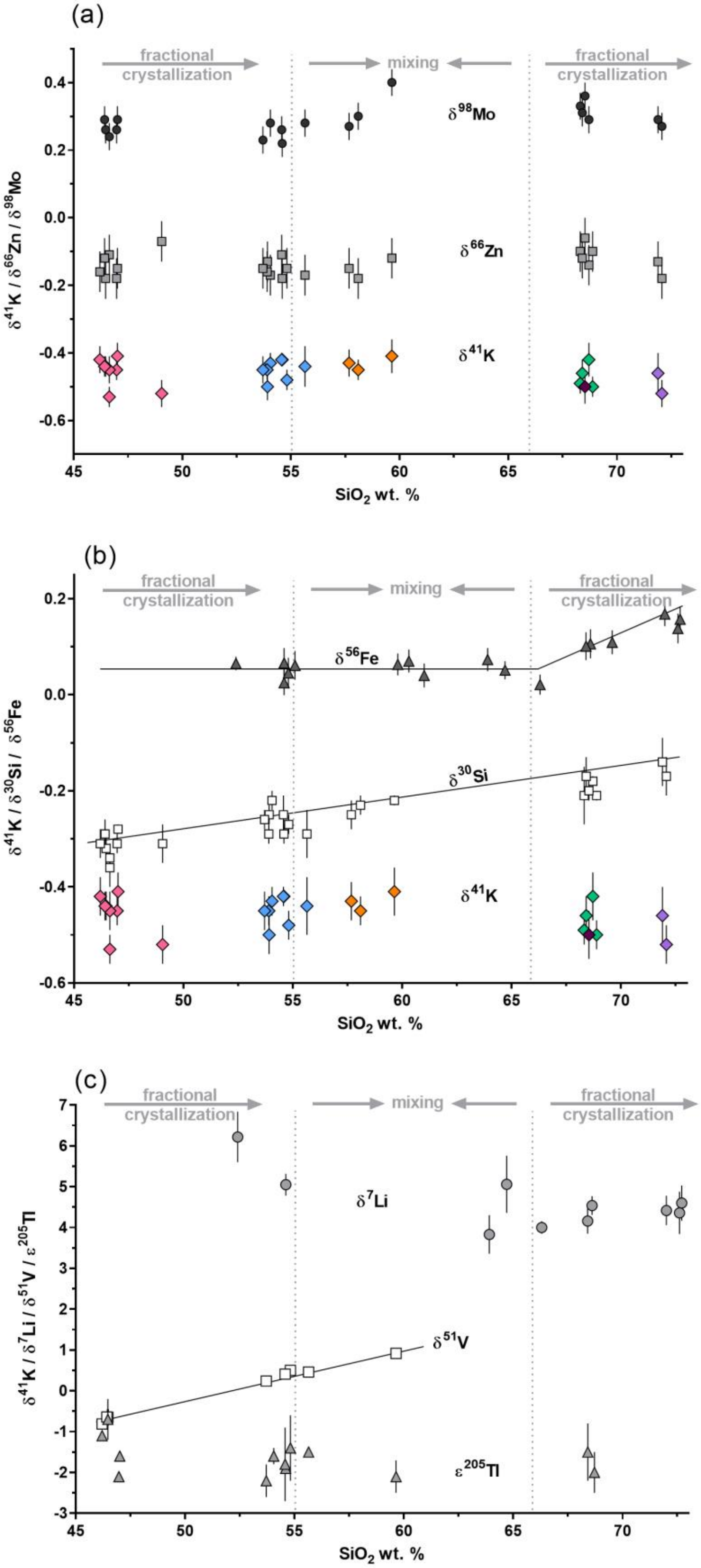
(a)
fractional crystallization
mixing
fractional crystallization
δ41K / δ66Zn / δ98Mo
0.4
0.2
0.0
-0.2
-0.4
-0.6
δ98Mo
δ66Zn
δ41K
45
50
55
60
65
70
SiO2 wt. %
(b)
fractional crystallization
mixing
fractional crystallization
δ41K / δ30Si / δ56Fe
0.2
0.0
-0.2
-0.4
-0.6
δ56Fe
δ30Si
δ41K
45
50
55
60
65
70
SiO2 wt. %
(c)
fractional crystallization
mixing
fractional crystallization
δ41K / δ7Li / δ51V / ε205Tl
7
6
5
4
3
2
1
0
-1
-2
-3
δ7Li
δ51V
ε205Tl
45
50
55
60
65
70
SiO2 wt. %

Figure 5: *K isotopic systematics of Hekla samples compared to a) other isotope systems showing no isotope fractionation at Hekla, namely Mo (Yang et al. 2018) and Zn (Chen et al. 2013); b) isotope systems showing clear fractionation trends, namely Fe (Schuessler et al. 2009) and Si (Savage et al. 2011); and c) Li isotopes (Schuessler et al. 2009), V isotopes (Prytulak et al. 2017), and Tl isotopes (Prytulak et al. 2016). Note that for Tl isotopes the notation is* ε^{205}*Tl so variation is exaggerated by a factor of 10.*

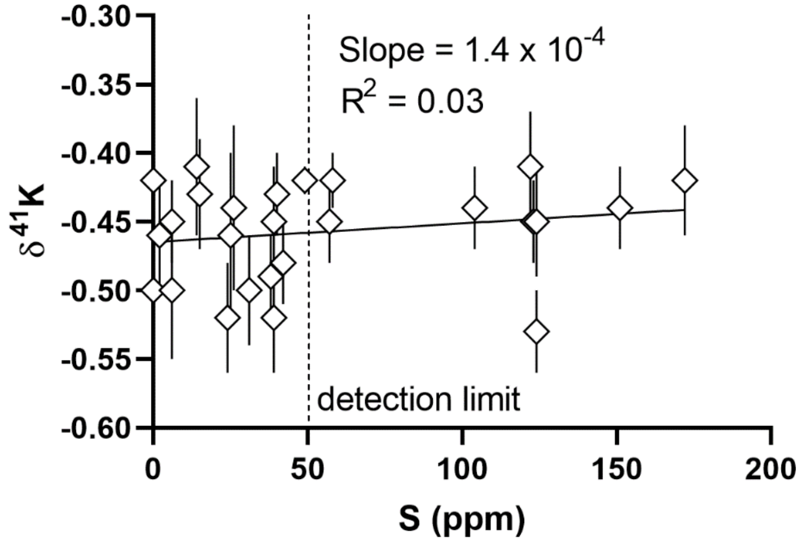

Figure 6: δ^{41}*K values for samples in this study plotted against their S concentration in ppm (from Savage et al. 2011). S detection limit was given as 50 ppm. Simple linear regression gives a slope of 0.00014 and* R^2*=0.03 indicating that the slope is not significantly non-zero.*

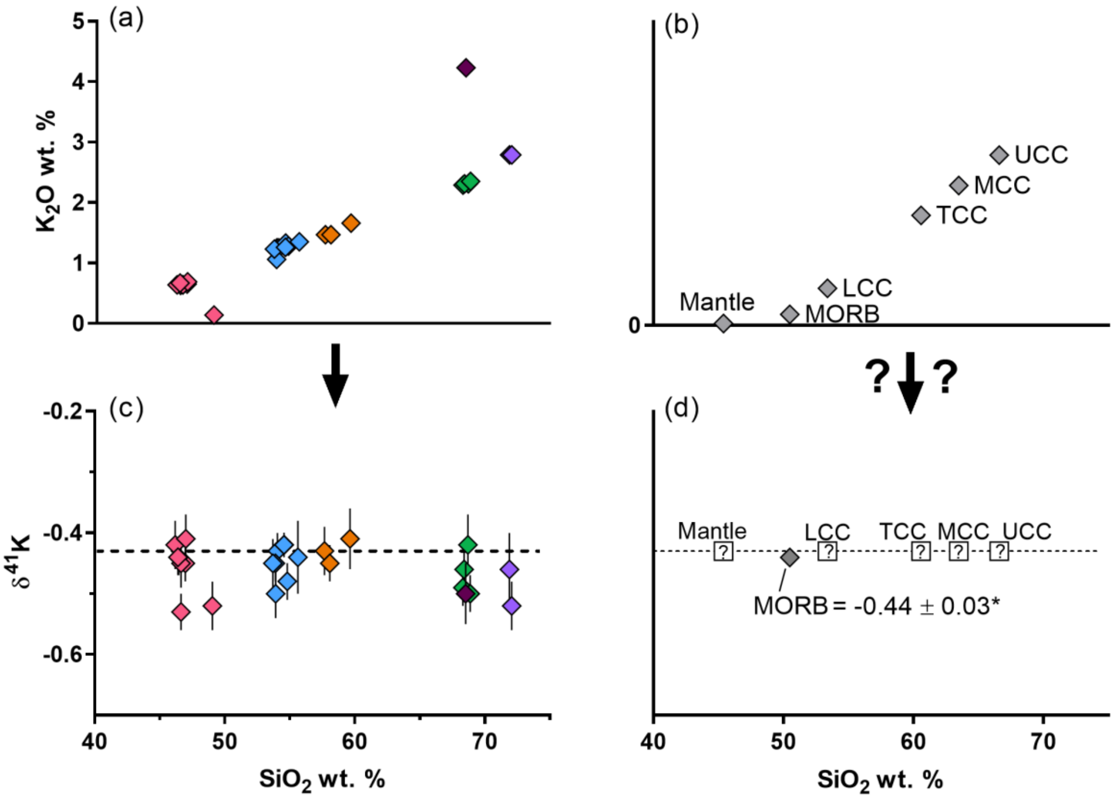

Figure 7: *Plot showing comparison between Hekla data and hypothesized Earth reservoir data, assuming only bulk K isotopic composition is considered. Panel (a) shows the potassium concentration of the Hekla samples versus their* SiO_2 *concentrations while panel (b) shows the same plot for the Earth reservoirs of the Mantle, MORBs, and the lower, middle, upper, and total continental crusts (LCC, MCC, UCC, and TCC, respectively); we can see the same rough trend in* SiO_2 *concentrations as in panel (a). Panel (c) shows the K isotopic composition of Hekla samples plotted against their* SiO_2 *concentrations; the zero slope indicates a lack of fractionation during magmatic differentiation as indicated by progressing* SiO_2 *values. Panel (d) illustrates how one might apply the pattern seen in the Hekla suite of samples to the greater suite of Earth reservoirs (bulk values). The gray dashed line indicates the BSE value of −0.43 taken from Tuller-Ross et al. (2019). It should be noted that the MORB value (−0.44; Tuller-Ross et al. 2019) is slightly below the dashed line because the BSE value of −0.43 was determined by an average of globally sourced MORBs, OIBs, and BABBs. OIBs in that study had an average of* $\delta^{41}K = -0.41 \pm 0.16$*, which, while statistically indistinguishable from the MORB value, contributed to increasing the average value by 0.01‰.*

Table 1. Potassium Isotopic Compositions of Hekla Samples

Sample	*Latitude (N)*	*Longitude (W)*	*Amount Dissolved (mg)*	*K_2O% (this study)*	*K_2O%*[a]	*$\delta^{41}K$ (‰)*	*95% c.i.*[b]	*n*[c]
Basalts								
HEK04-09	64°04'24.3"	19°31'14.8"	11.6	0.62	0.65	−0.45	0.03	12
HEK05-09	64°04'14.2"	19°25'21.8"	13.5	0.61	0.63	−0.44	0.03	12
HEK06-09	64°04'03.6"	19°24'45.5"	11.8	0.61	0.64	−0.42	0.04	12
HEK07-09	64°03'56.2"	19°31'55.8"	10.0	0.66	0.64	−0.45	0.04	11
HEK07-09c	64°03'56.2"	19°31'55.8"	15.6	0.62	0.64	−0.53	0.03	10
HEK09-09	64°01'01.9"	19°31'27.3"	14.4	0.69	0.69	−0.41	0.04	10
HEK12-09	63°59'19.3"	19°31'56.5"	12.8	0.64	0.67	−0.44	0.03	10
Basaltic Andesites								
HEK02-09	64°04'34.7"	19°36'57.0"	16.1	1.23	1.25	−0.50	0.04	11
HEK03-09	64°04'35.8"	19°36'54.4"	14.3	1.18	1.25	−0.43	0.03	10
HEK08-09	64°01'36.9"	19°36'06.1"	10.2	1.28	1.33	−0.42	0.01	11
HEK13-09	63°58'10.5"	19°34'12.0"	16.8	1.16	1.06	−0.45	0.03	10
HEK14-09	63°57'38.6"	19°35'27.8"	12.8	1.18	1.23	−0.45	0.04	10
HEK16-09	64°00'22.1"	19°36'57.1"	11.4	1.09	1.28	−0.48	0.03	10
HEK17-09	64°00'21.2"	19°36'58.7"	11.9	1.22	1.26	−0.42	0.02	11
HEK21-09	63°56'27.8"	19°56'56.8"	10.6	1.28	1.35	−0.44	0.06	9
Andesites								
HEK10-09	63°59'27.6"	19°33'55.0"	10.8	1.47	1.47	−0.43	0.04	10
HEK11-09	63°59'23.1"	19°33'00.4"	14.6	1.36	1.47	−0.45	0.03	10
HEK15-09	64°00'21.1"	19°36'43.9"	15.0	1.67	1.66	−0.41	0.05	10
Dacites (tephra)								
HEK01-09	64°03'50.7"	19°46'31.2"	15.8	2.45	2.31	−0.42	0.05	10
HEK02-10	64°03'55.0"	19°40'02.9"	10.8	2.44	2.29	−0.49	0.03	10
HEK18-09	64°03'58.5"	19°45'50.7"	11.5	2.19	2.31	−0.46	0.04	11
HEK19-09	64°03'58.5"	19°45'50.7"	11.2	2.33	2.34	−0.50	0.03	10
Rhyolites (tephra)								
HEK01-10	64°04'31.7"	19°38'36.0"	11.7	2.81	2.79	−0.46	0.06	11
HEK03-10	64°04'24.7"	19°38'52.5"	10.7	2.75	2.79	−0.52	0.04	12
Burfell samples								
BUR20-09	(basalt)		16.0	0.13	0.14	−0.52	0.04	12
RHY01-09	(trachyte)		12.2	4.39	4.23	−0.50	0.05	11
External Standard								
BHVO-2						−0.47	0.02	32

[a] K_2O% from Savage et al. 2011;

[b] 95% confidence interval (c.i.); z × [$\sigma/\sqrt{(n-1)}$], where z is the student's t number, σ = standard deviation, and n = number of runs

[c] n= number of runs.

Highlights

- We measured K isotopes of a series of cogenetic igneous rocks from Hekla, Iceland
- No resolvable K isotopic variations among volcanic rocks from basalt to rhyolite
- K isotopes are likely not fractionated during igneous differentiation processes
- Data agrees with prior estimates for the bulk K isotope composition of the mantle

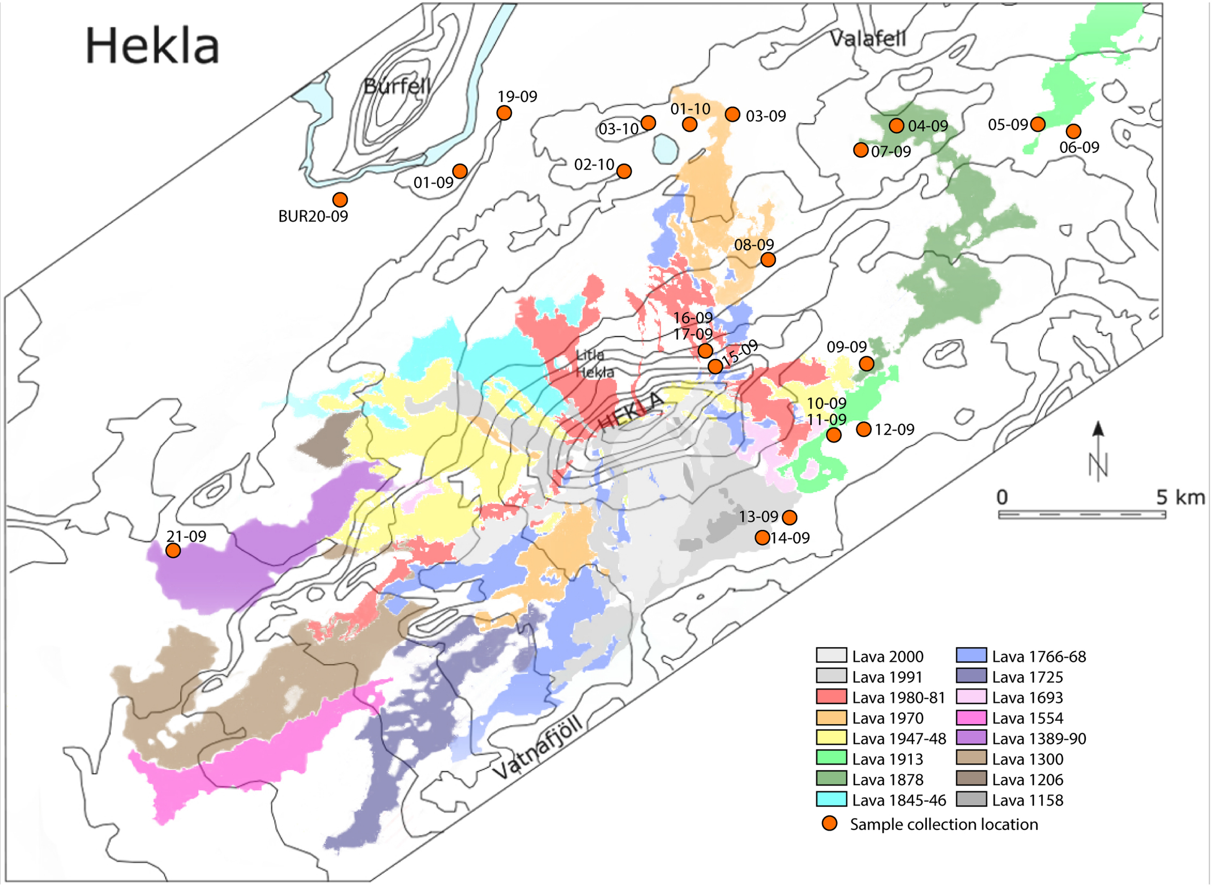
Hekla
Búrfell
Valafell
19-09
01-10
03-09
03-10
04-09
05-09
06-09
07-09
02-10
01-09
BUR20-09
08-09
16-09
17-09
15-09
09-09
Litla Hekla
HEKLA
10-09
11-09
12-09
13-09
14-09
21-09
Vatnafjöll
N
0
5 km
Lava 2000
Lava 1991
Lava 1980-81
Lava 1970
Lava 1947-48
Lava 1913
Lava 1878
Lava 1845-46
Lava 1766-68
Lava 1725
Lava 1693
Lava 1554
Lava 1389-90
Lava 1300
Lava 1206
Lava 1158
Sample collection location

Figure 1

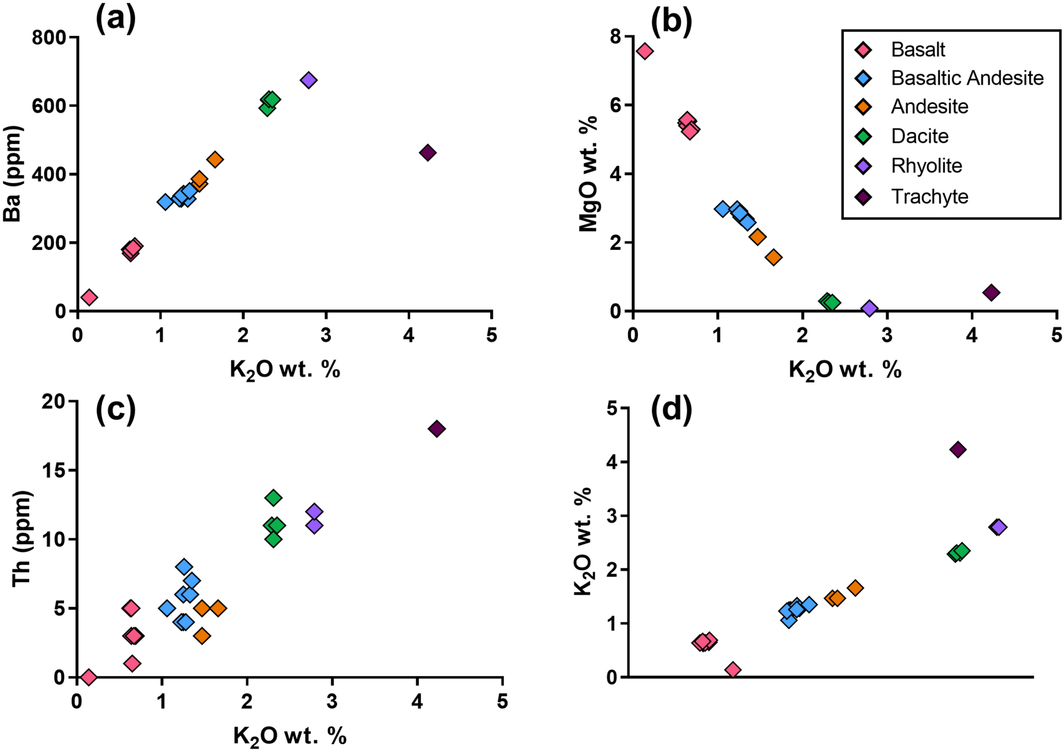
(a)
Ba (ppm)
800
600
400
200
0
0
1
2
3
4
5
K$_2$O wt. %
(b)
MgO wt. %
8
6
4
2
0
0
1
2
3
4
5
K$_2$O wt. %
Basalt
Basaltic Andesite
Andesite
Dacite
Rhyolite
Trachyte
(c)
Th (ppm)
20
15
10
5
0
0
1
2
3
4
5
K$_2$O wt. %
(d)
K$_2$O wt. %
5
4
3
2
1
0

Figure 2

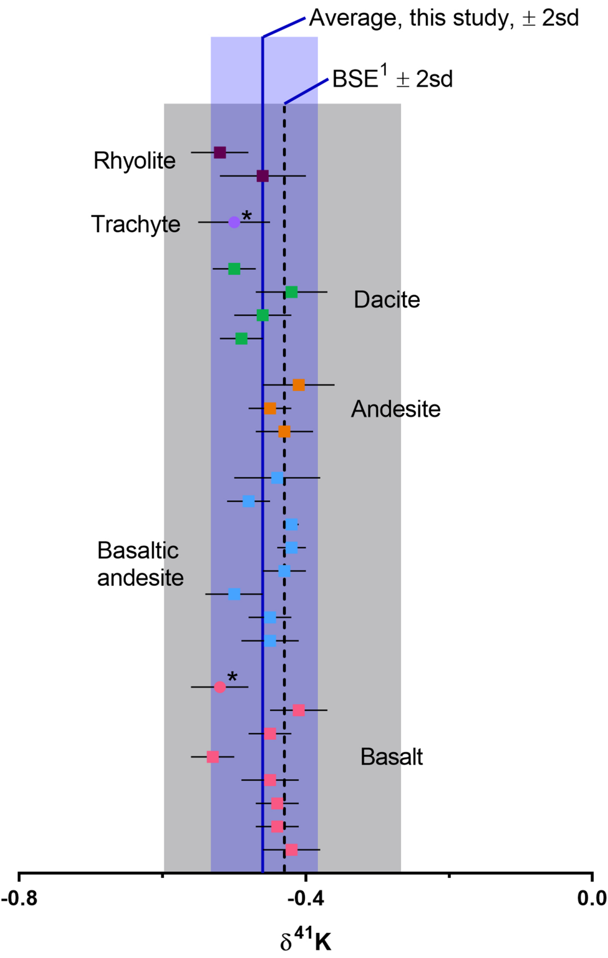
Average, this study, ± 2sd
BSE1 ± 2sd
Rhyolite
Trachyte
*
Dacite
Andesite
Basaltic andesite
*
Basalt
-0.8
-0.4
0.0
δ41K

Figure 3

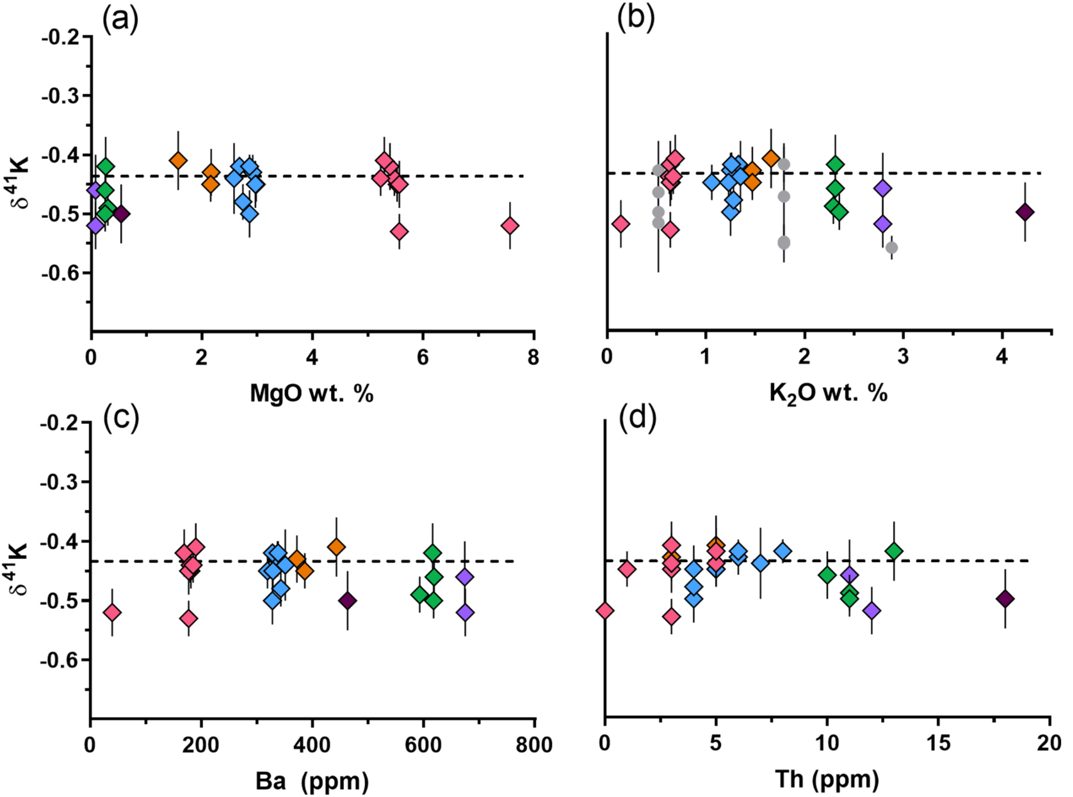
(a)
(b)
(c)
(d)
δ^{41}K
-0.2
-0.3
-0.4
-0.5
-0.6
MgO wt. %
0
2
4
6
8
K_2O wt. %
0
1
2
3
4
Ba (ppm)
0
200
400
600
800
Th (ppm)
0
5
10
15
20

Figure 4

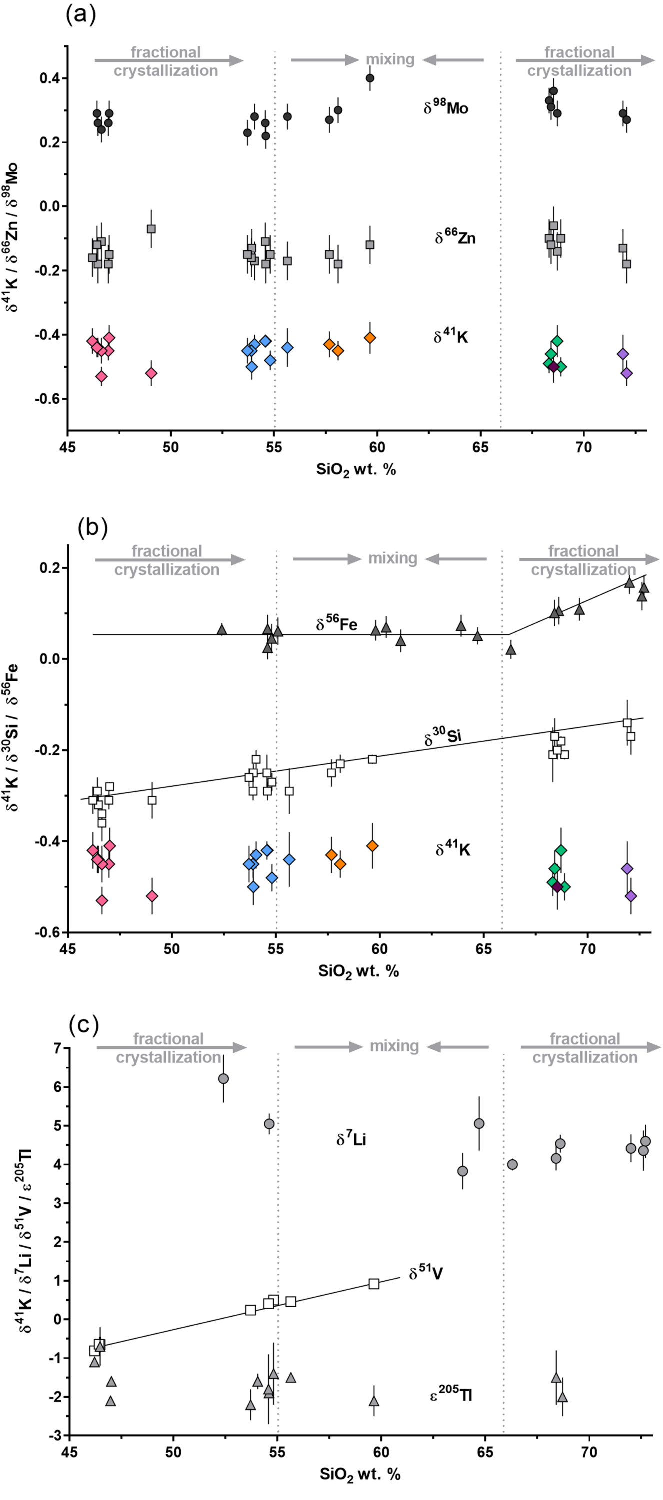
(a)
fractional crystallization
mixing
fractional crystallization
δ^{98}Mo
δ^{66}Zn
δ^{41}K
δ^{41}K / δ^{66}Zn / δ^{98}Mo
0.4
0.2
0.0
-0.2
-0.4
-0.6
45
50
55
60
65
70
SiO$_2$ wt. %
(b)
fractional crystallization
mixing
fractional crystallization
δ^{56}Fe
δ^{30}Si
δ^{41}K
δ^{41}K / δ^{30}Si / δ^{56}Fe
0.2
0.0
-0.2
-0.4
-0.6
45
50
55
60
65
70
SiO$_2$ wt. %
(c)
fractional crystallization
mixing
fractional crystallization
δ^{7}Li
δ^{51}V
ε^{205}Tl
δ^{41}K / δ^{7}Li / δ^{51}V / ε^{205}Tl
7
6
5
4
3
2
1
0
-1
-2
-3
45
50
55
60
65
70
SiO$_2$ wt. %

Figure 5

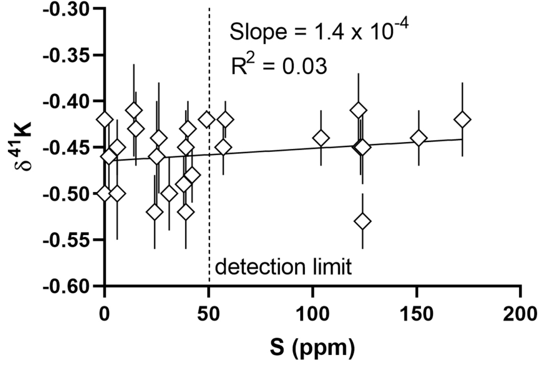
Slope = 1.4 x 10^{-4}
R^2 = 0.03
detection limit
δ^{41}K
-0.30
-0.35
-0.40
-0.45
-0.50
-0.55
-0.60
0
50
100
150
200
S (ppm)

Figure 6

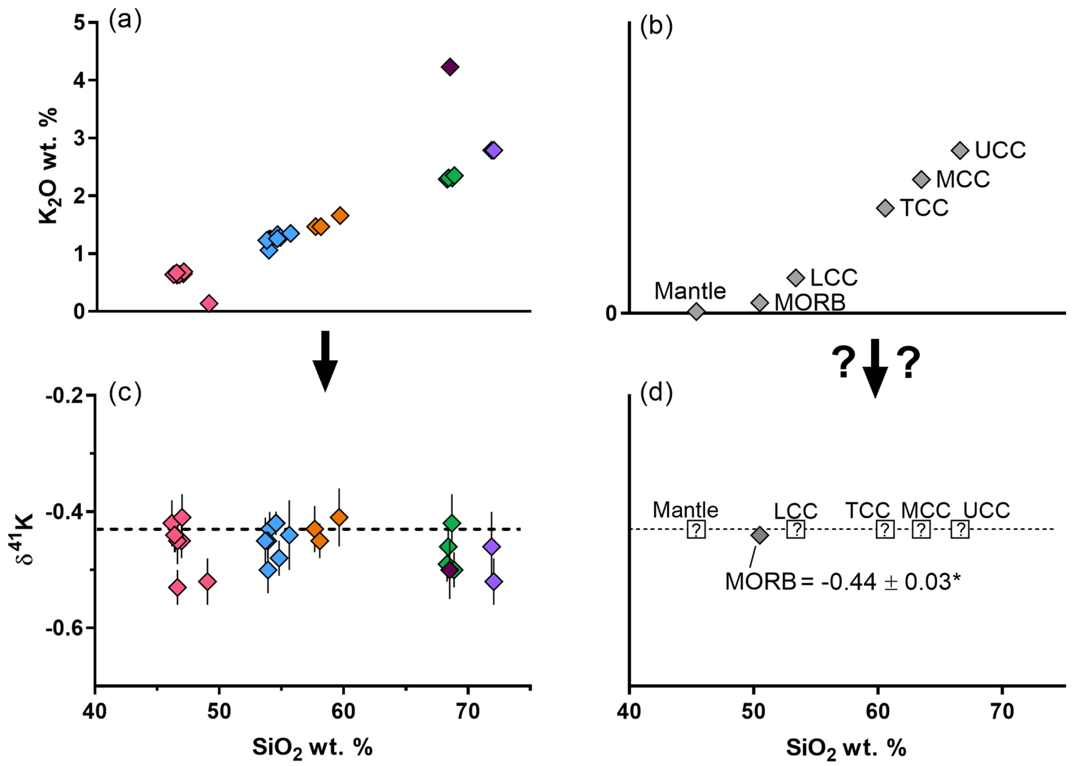
(a)
K2O wt. %
5
4
3
2
1
0
(b)
UCC
MCC
TCC
LCC
Mantle
MORB
0
? ?
(c)
δ41K
-0.2
-0.4
-0.6
40
50
60
70
SiO2 wt. %
(d)
Mantle
LCC
TCC
MCC
UCC
?
MORB = -0.44 ± 0.03*
40
50
60
70
SiO2 wt. %

Figure 7